IN VIVO CONSTRUCTION OF A NANOREACTOR USING CHARGE COMPLEMENTARITY

by

Seung Ook Yang

A thesis submitted to the faculty of
The University of Utah
in partial fulfillment of the requirements for the degree of

Master of Science

Department of Chemistry

The University of Utah

December 2012

The University of Utah Graduate School

STATEMENT OF THESIS APPROVAL

The following faculty members served as the supervisory committee chair and members for the thesis of **Seung Ook Yang**.

Dates at right indicate the members' approval of the thesis.

Kenneth J. Woycechowsky, Chair	**10/25/2012** Date Approved
Bethany A. Koehntop, Member	**10/25/2012** Date Approved
Cynthia Burrows, Member	**10/25/2012** Date Approved

The thesis has also been approved by **Henry S. White**, Chair of the Department/School/College of **Chemistry**

and by Charles A. Wight, Dean of The Graduate School.

ABSTRACT

Subcellular protein compartmentalization is one of the strategies that nature has adapted for various functions, such as storage and protection of cargo molecules as well as regulation of chemical reactions. There is a growing interest among nanotechnologists to utilize protein capsids for encapsulating guest molecules in bioimaging, drug-delivery, nanoreactors, etc. To date, many viral and nonviral protein capsids have been investigated for those applications.

We used an engineered an *Aquifex aeolicus* lumazine synthase variant (AaLS-13) as a platform to encapsulate a guest enzyme by charge complementarity. The enzyme, esterase Est55 bearing a C-terminal deca-arginine (R_{10}) tag, was placed in the lumen of the AaLS-13 during the self-assembly of the capsid when co-produced in *E. coli*. This encapsulated enzyme was characterized by colorimetric assay with the substrate, p-nitrophenyl acetate. Comparison of the specific esterase activity between the empty capsid and the enzyme-loaded capsid showed 64-fold higher specific activity in the enzyme-loaded capsid compared to the empty capsid. Mass spectrometry and proteomics analysis verified that the presence of Est55-R_{10} in a sample of purified AaLS-13 that had been co-produced with the esterase. Capsid loading was estimated by esterase activity measurements and SDS-PAGE analysis. Both methods gave a loading estimate of one esterase molecule per eleven capsids.

We plan to improve capsid loading using "supercharged" esterases. We also plan to investigate the porosity of the capsid because size limit for small molecule diffusion in and out of capsid is not well defined. Esterase substrates of various sizes will be applied to both esterase-loaded capsid and free esterase to determine the molecular weight cut-off of the AaLS-13 capsid.

TABLE OF CONTENTS

LIST OF FIGURES

LIST OF TABLES

LIST OF ABBREVIATIONS

AaLS	*Aquifex aeolicus* lumazine synthase
BsLS	*Bacillus subtilis* lumazine synthase
Est55	*Geobacillus stearothermophilus* esterase
FPLC	Fast protein liquid chromatography
GFP	Green fluorescence protein
IPTG	Isopropyl β-D-1-thiogalactopyranoside
Ni^{2+}-NTA	Nickel-nitrilotriacetic acid
OD	Optical density
R_{10}	A deca arginine tag
SDS-PAGE	Sodium dodecyl sulfate polyacrylamide gel electrophoresis

ACKNOWLEDGEMENTS

I would first and foremost like to thank my advisor, Professor Ken Woycechowsky, for all his guidance, encouragement, passion, ideas, and knowledge that he has shared with me during my time in the graduate program. He has been a role model to me both as a successful research scientist and an excellent leader. He has been always there for me whenever questions and problems arise.

I would like to thank the Woycechowsky group members, Chen, Geoff, Larry, Emily, Monica, and Mark, for all their support, great memories, and learning experiences. I want to thank the Department of Chemistry at the University of Utah, particularly the members of my committee; Jim Muller and Chad Nelson for their help and knowledge; and Jo Hoovey and Katie Shelton for all their hard work in keeping the department running.

I would finally like to thank my family and friends. Words cannot fully express my gratitude and love to them for all of their support, encouragement, advice, and love they have given me over the years. I would not be where I am today without them.

CHAPTER 1

INTRODUCTION

Icosahedral protein capsids are highly symmetric structures that enclose a central cavity, which isolates the interior environment from the bulk solution.[1] These soccer ball-like structures are often the product of self-assembly by multiple identical subunits. Viruses provide many examples of such protein cages, in which the viral capsid secures and carries its infectious genetic information. Protein capsids are not limited to viruses, and in nature these assemblies often encapsulate enzymes to function as nanoscale reaction vessels. Such reactions include carbon fixation, propanediol utilization, and ethanolamine utilization.[2]

The ethanolamine utilization bacterial microcompartment is one of the most extensively studied natural nanoreactors. A major role of this subcellular microcompartment is to produce energy via the action of encapsulated guest enzymes, which convert the substrate, ethanolamine to acetyl CoA and ethanol. The potentially toxic intermediate, acetaldehyde, is not released into the cytosol because its high local concentration in the capsid promotes efficient capture by enzyme active sites, and the tightly packed protein shell presents a barrier to diffusion of the intermediate into bulk solution. The microcompartment has gated pores as well that selectively allow its

substrate to penetrate the protein shell[3] in response to cellular conditions. Thus the enzyme activity is enhanced and regulated.

Natural molecular containers can also be useful for nanotechnology. Their narrow size distribution and easy modification by genetic methods make protein capsids particularly attractive as platforms for nanotechnological applications. To date, viral and non-viral self-assembled protein cages have been employed as delivery vehicles,[4-7] bioimaging agents,[8-11] inorganic nanoparticle synthesis vessels,[12,13] and nanoreactors[14-16].

Demands for employment of enzymes and whole cells as biocatalysts have been increased in industries such as foods, drinks, fine chemicals, etc. Biotechnologists want to develop efficient enzyme catalysts that can be regulated in a sophisticated manner. Although there have been several attempts to build nanoreactors with proteinaceous,[10-12] liposomal,[17] and dendritic[18] containers, none of them are necessarily designed to regulate enzyme activity in a systematic manner. Here, we aim to construct an artificial bio-inspired nanoreactor in which an esterase enzyme acts as the guest and a bacterial protein capsid acts as the host.

1.1 Capsid Protein: Lumazine Synthase from *Aquifex aeolicus* (AaLS)

The capsid formed by lumazine synthase (AaLS) is a particularly promising scaffold for developing novel encapsulation systems. It is an enzyme that catalyzes the penultimate step of riboflavin synthesis (Figure 1.1). AaLS forms a hollow icosahedral capsid by self-assembly with 60 identical subunits. This capsid is highly thermostable with the melting temperature of 120 °C.[19]

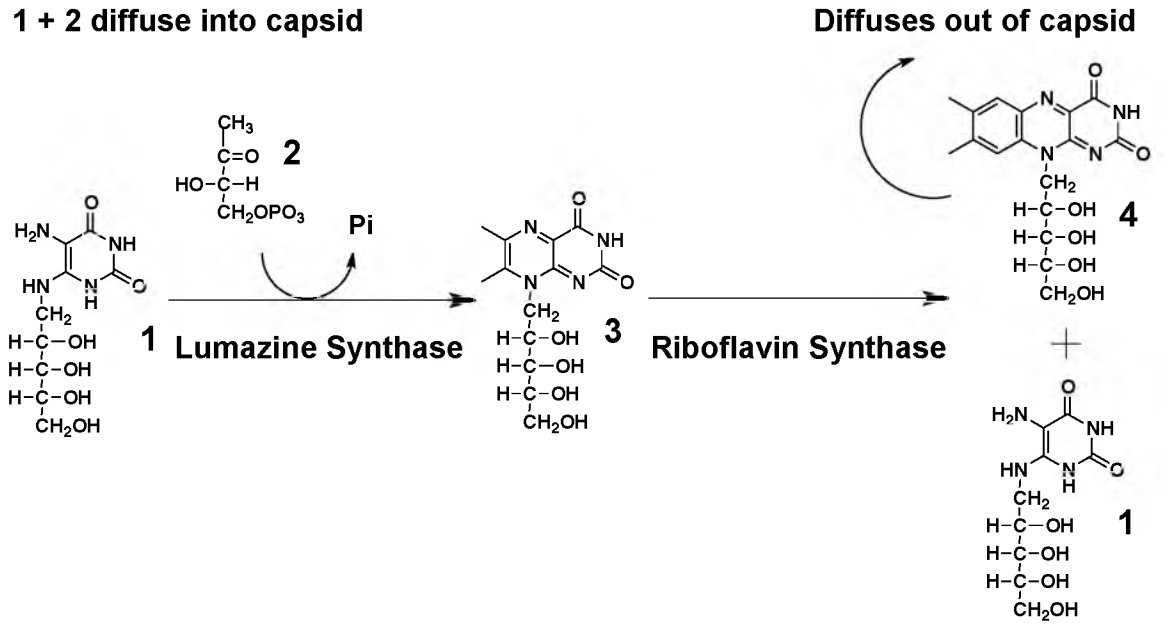

Figure 1.1. Riboflavin synthesis by the lumazine synthase/riboflavin synthase complex. **1**, 5-amino-6-ribitylamino-2,4(1H,3H)-pyrimidinedione; **2**, 3,4-dihydroxy-2-butanone; **3**, 6,7-dimethyl-8-ribityllumazine; **4**, riboflavin.

The AaLS capsid has pores located at every five-fold symmetry axis. The pore has a roughly cylindrical shape with a relatively wide opening at the inner and the outer surfaces whereas halfway in between the pore is narrower. The pore is believed to serve as a tunnel for the substrates that have to penetrate the capsid and interact with the active site, which is located at the inner surface of the capsid.

Questions have been raised for many years as to how the substrate can arrive at the active site of the capsid and how the product can diffuse out. A homologous lumazine synthase from *Bacillus subtilis* (BsLS) also forms a capsid with 60 identical subunits, but BsLS is known to orchestrate riboflavin biosynthesis by encapsulating riboflavin synthase, a 66 kDa homotrimeric enzyme. An early modeling study revealed that the five-fold symmetric pore does provide sufficient space for passage of riboflavin out of

the capsid.[20] However, it is not possible for a bulky riboflavin to diffuse out through the capsid pore without violating energetic criteria of the protein structure.[21] This latter hypothesis suggests that alternative pores may exist in the capsid that are not apparent in the X-ray structure. As the porosity of the capsid is not well characterized, it is worthwhile to recount porosity of the capsid and to determine molecular weight cut-off for substrates.

Previously, AaLS has been engineered to encapsulate guest proteins by charge complementarity (Figure 1.2). On the interior surface of the wild type capsid, four of the most solvent accessible residues of a monomer have been mutated to glutamate. This mutated capsid is named AaLS-neg. Interestingly, the diameter of the mutated capsid is 27 nm whereas that of wild type AaLS (AaLS-wt) is 16 nm. The AaLS-neg capsid assembles from 180 subunits rather than 60 subunits. Thus, AaLS-neg bears 720 additional negative charges in the lumen of the capsid. AaLS-neg has been co-produced with a deca-arginine tagged GFP (GFP-R_{10}) in *E. coli*. The capsids contain 3-4 GFP-R_{10} molecules on average.[22] AaLS-neg has been further engineered to enhance its loading capacity. Directed evolution of AaLS-neg to optimize its ability to encapsulate HIV-protease-R_{10} led to the selection of variant AaLS-13 containing five additional mutations at the subunit interfaces and two additional mutations at the interior surface. This time, an even bigger capsid has been formed with the diameter of 35 nm. AaLS-13 was found to encapsulate an average of seven HIV-protease-R_{10} dimers per capsid as measured by Western blot.[23]

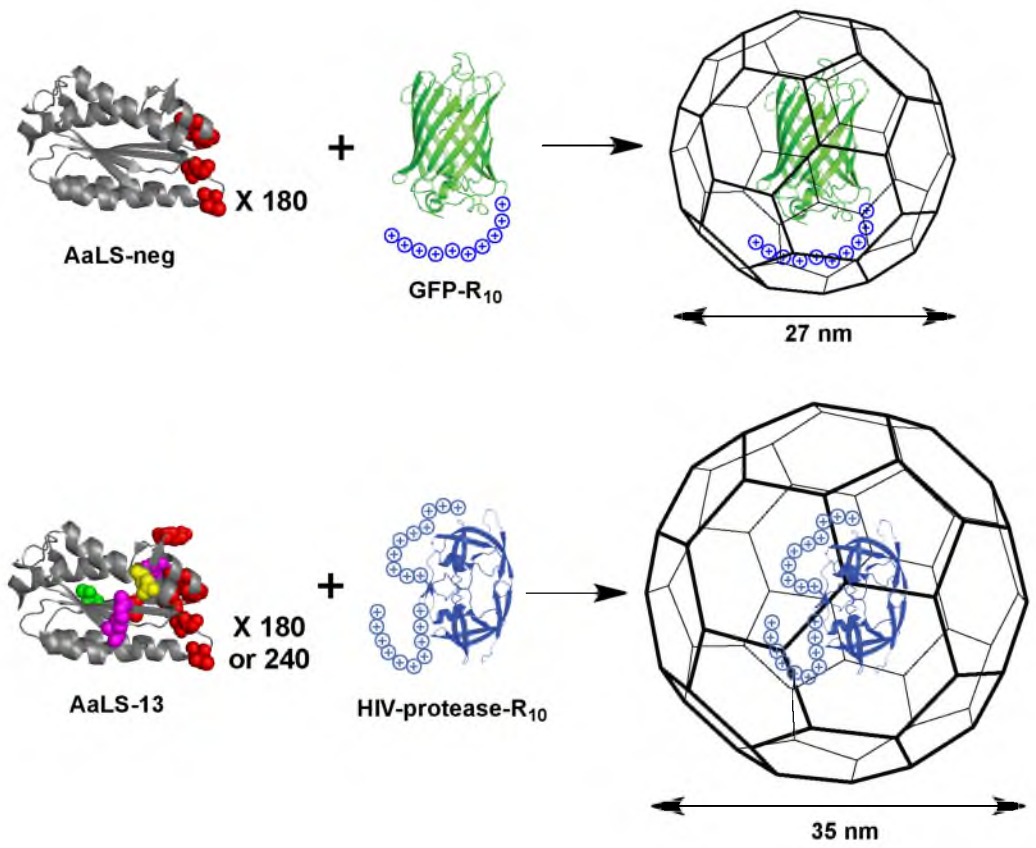

Figure 1.2. Encapsulation of guest molecules by AaLS capsid variants by charge complementarity. Rational design for AaLS-neg (R83E, T86E, T120E, and Q123E) and directed evolution for AaLS-13 (D28G, R52C, T112S, V115D, A118D, R127C and K131E) made it possible for the capsid to expand with enhanced guest molecule loading capacity. The colors used in the description of the mutations above corresponds to the highlighted residues in the structures of the AaLS-neg and AaLS-13 monomers shown in the figure.

According to the model for guest encapsulation shown in Figure 1.2, the guest enzyme should be in an active state. However it was not possible to detect the catalysis of the guest enzyme because the protease was not active at pH 8 where the capsid is stable, the capsid was not soluble below pH 6 where the protease is most active, and the substrates for the enzyme might have been too big to penetrate the capsid.[24] Therefore, a new guest is needed to study catalysis of enzymes encapsulated by AaLS-13.

1.2 A New Guest Enzyme: Carboxylesterase (Est55)

The goal of this project is to study the influence of encapsulation on enzyme activity. The enzyme for the encapsulation system was carefully selected using the following five criteria. First, the enzyme should not contain disulfide bonds. Any disulfide bond will likely be reduced due to the reducing conditions in cytoplasm where the enzyme and the capsid are produced and assembled. Second, the enzyme should be independent from any cofactors. It is easier to assay an enzyme that can stand-alone, additionally problems may arise with the entry of cofactors into capsid pores. Third, the pH-rate profile of the enzyme should be known. The enzyme should show optimum activity near pH 8 to ensure compatibility with the capsid. Fourth, a convenient and sensitive assay for enzyme activity is required. Lastly, the encapsulated enzyme should have broad substrate specificity to permit experiments involving variations in substrate structure.

A carboxylesterase (Est55) from *Geobacillus Stearothermophilus* meets these criteria and was chosen to be the guest enzyme for these studies. Carboxylesterases have been shown catalyze the hydrolysis of a variety of substrates.[25-28] Importantly, Est55 has a reported maximum activity at pH 8,[26] which is the same pH at which previous studies with AaLS-13 have been carried out. A R_{10}-tag has been fused to the C-terminus of Est55 (Est55-R_{10}) to promote its encapsulation in AaLS-13 upon co-production.[29] The crystal structure of Est55 clearly shows that the C-terminus is remote from the active site on the opposite side of the enzyme (Figure 1.3), which is important because R_{10}-tag may interfere the catalysis of the enzyme if they are close to each other.

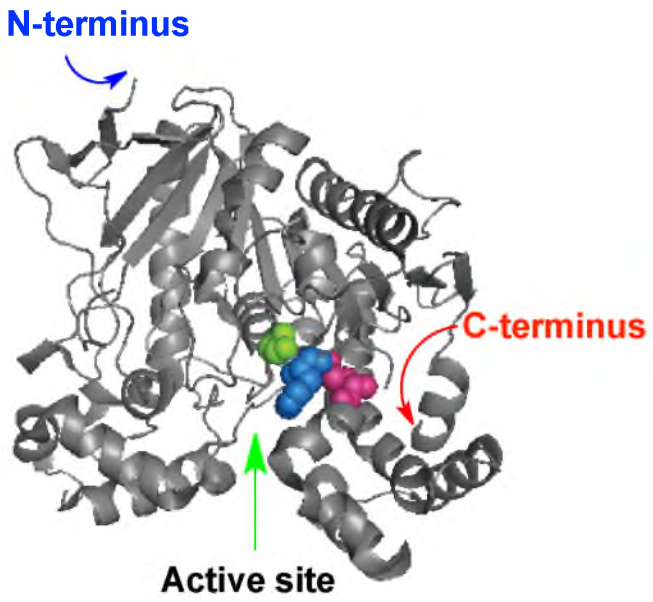

Figure 1.3. Crystal structure of esterase (Est55). Est55 is a part of α/β hydrolase fold family. The active site contains catalytic triad with residues of Ser194, Glu310, and His409. The colors used in the list of the catalytic triad residues corresponds to the colors of the residues highlighted in the Est55 structure shown in the figure.

CHAPTER 2

RESULTS

Most enzyme activity measurements are done in bulk solution. However, sequestration of enzymes in nanocompartments can enhance the stability of enzymes and provide opportunities for activity regulation. As a proof of principle, we designed a bio-inspired enzyme encapsulation system by charge complementarity. We aim to study the activity of encapsulated enzymes in comparison with free enzymes.

2.1 Stability of AaLS-13

Capsid stability is an important feature for nanoreactor applications. AaLS-13 has been constructed by rational design and directed evolution.[22,24] As mutations have been introduced at subunit interaction sites in the capsid, it decreased the thermal stability of the capsid. Further, production of the capsid in the absence of R_{10}-tagged guest proteins leads to a mixture of properly assembled capsid and incompletely assembled capsid fragments. We wanted to know if the quaternary structure is prone to spontaneous disassembly. Three samples of AaLS-13 were produced in parallel *E. coli* cultures. The harvested cells were lysed and purified by an affinity column. Further purification of the three AaLS-13 protein samples was done by size exclusion chromatography on the same

day. Capsid-containing fractions for each of the three samples were pooled, concentrated to 1.5 mg/mL, and stored at 4 °C. Every 10 days, one of the samples was reinjected onto the size exclusion column. Over a total of 30 days, the chromatograms showed only minor differences, which indicate that the AaLS-13 capsid structure maintains a high quaternary structure resilience (Figure 2.1).

2.2 Activity of Free Est55-R_{10}

p-Nitrophenyl acetate was used as a model substrate to measure esterase activity because it should be small enough to enter the capsid, the reaction could be monitored by a colorimetric assay ($\Delta\varepsilon_{405nm}$ = 17800 $M^{-1}cm^{-1}$), and Est55 has been previously shown to efficiently hydrolyze the substrate.[26]

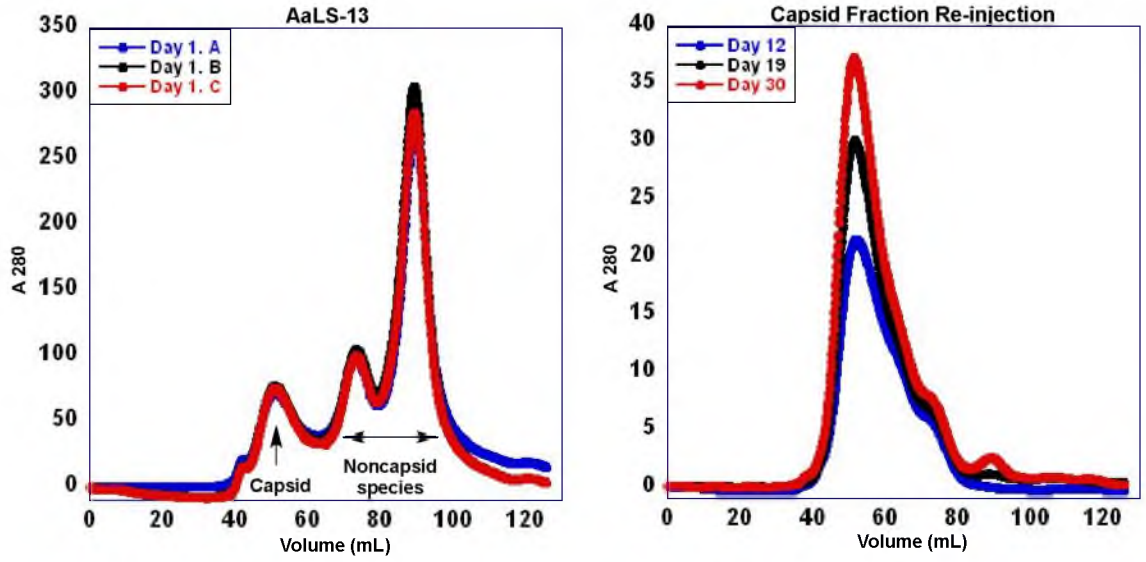

Figure 2.1. AaLS-13 stability. Size exclusion chromatograms showed the quaternary structure of the capsid did not change over 30 days. Left: Chromatograms for the identical AaLS-13 samples injected immediately following Ni^{2+}NTA affinity purification. Right: Chromatograms for the re-injection of each sample from left after the indicated incubation time.

Michaelis-Menten kinetic analysis of Est55-R_{10} gave k_{cat}, K_m, and k_{cat}/K_m values of 910 s^{-1}, 350 μM, and 2.6 x 10^6 $M^{-1}s^{-1}$, respectively. These data confirm that Est55-R_{10} efficiently hydrolyzes p-nitrophenyl acetate under our standard buffer conditions (Figure 2.2). Kinetic assays at higher substrate concentrations were not feasible because of the solubility limit of the substrate in the assay buffer (0.5 % ethanol). Higher concentrations of a co-solvent that increased substrate solubility were detrimental to the activity of Est55-R_{10} (data not shown). Most importantly, these results indicated that Est55-R_{10} is a promising guest enzyme for our encapsulation studies.

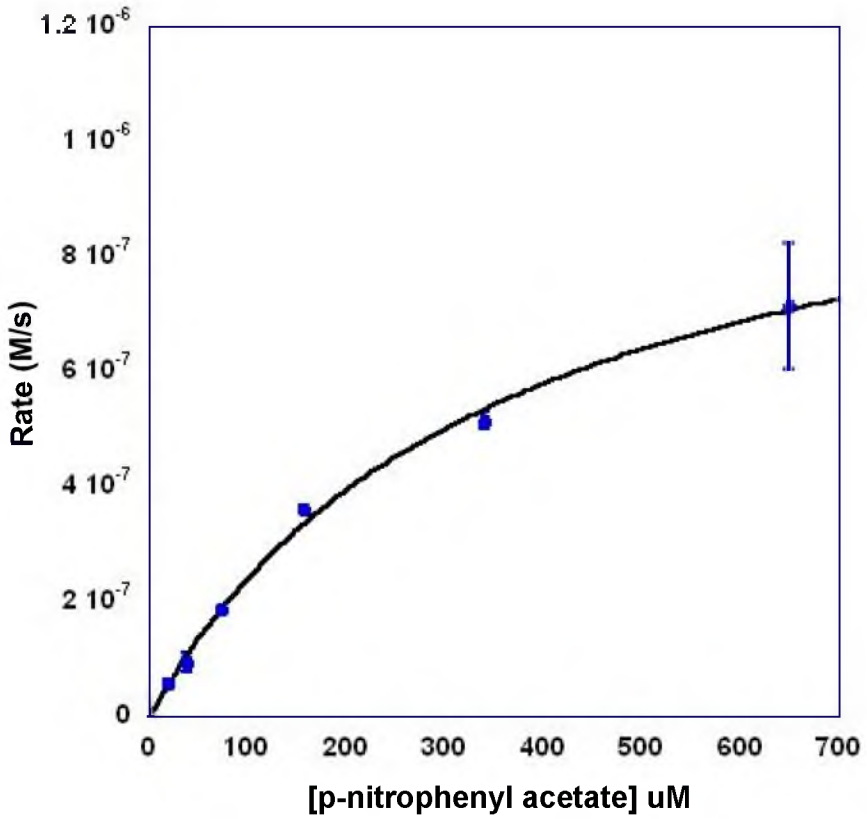

Figure 2.2. Michaelis-Menten kinetics of free Est55-R_{10}. At [Est55-R10] = 1.2 nM, pH = 8.0, T = 30 °C, V_{max} was determined to be 1.1 x 10^{-6} M/s from a fit of the data to the Michaelis-Menten equation.

2.3 Enzyme Encapsulation (Protein Production and Purification)

To generate an encapsulation complex of AaLS-13 and Est55-R_{10}, the two proteins were co-produced in *E. coli*. In this co-production system, the genes encoding AaLS-13 and Est55-R_{10} were on separate plasmids, with both under the control of identical dual T7-salicylate promoter systems. Sodium dodecyl sulfate polyacrylamide gel electrophoresis (SDS-PAGE) analysis showed that over-production of both AaLS-13 and Est55-R_{10} was induced by Isopropyl β-d-1-thiogalactopyranoside (IPTG) and salicylate, respectively (Figure 2.3). Unfortunately, upon co-production, the yield of Est55-R_{10} was substantially lower than the yield of AaLS-13. This relatively poor production of Est55-R_{10} could be explained by either Est55-R_{10}-associated toxicity to *E. coli* or sub-optimal induction conditions. The toxicity hypothesis was tested by producing Est55-R_{10} alone. However, under these conditions, esterase production increased suggesting that the esterase is not very toxic to *E. coli*. An attempt was made to optimize co-production by systemically varying induction conditions such as the concentration of IPTG, concentration of salicylate, induction time, temperature, and the ratio of IPTG concentration to salicylate concentration. However, none of these changes significantly improved co-production. Therefore, we carried out the encapsulation studies using the standard co-production conditions mentioned in Materials and Methods.

2.4. Enzyme Activity of Loaded Capsid vs Empty Capsid

After the affinity column purification, the AaLS-13 that was co-produced with Est55-R_{10} was further purified by size-exclusion chromatography. In comparison with AaLS-13 produced in the absence of Est55-R_{10}, co-production with the esterase gave a

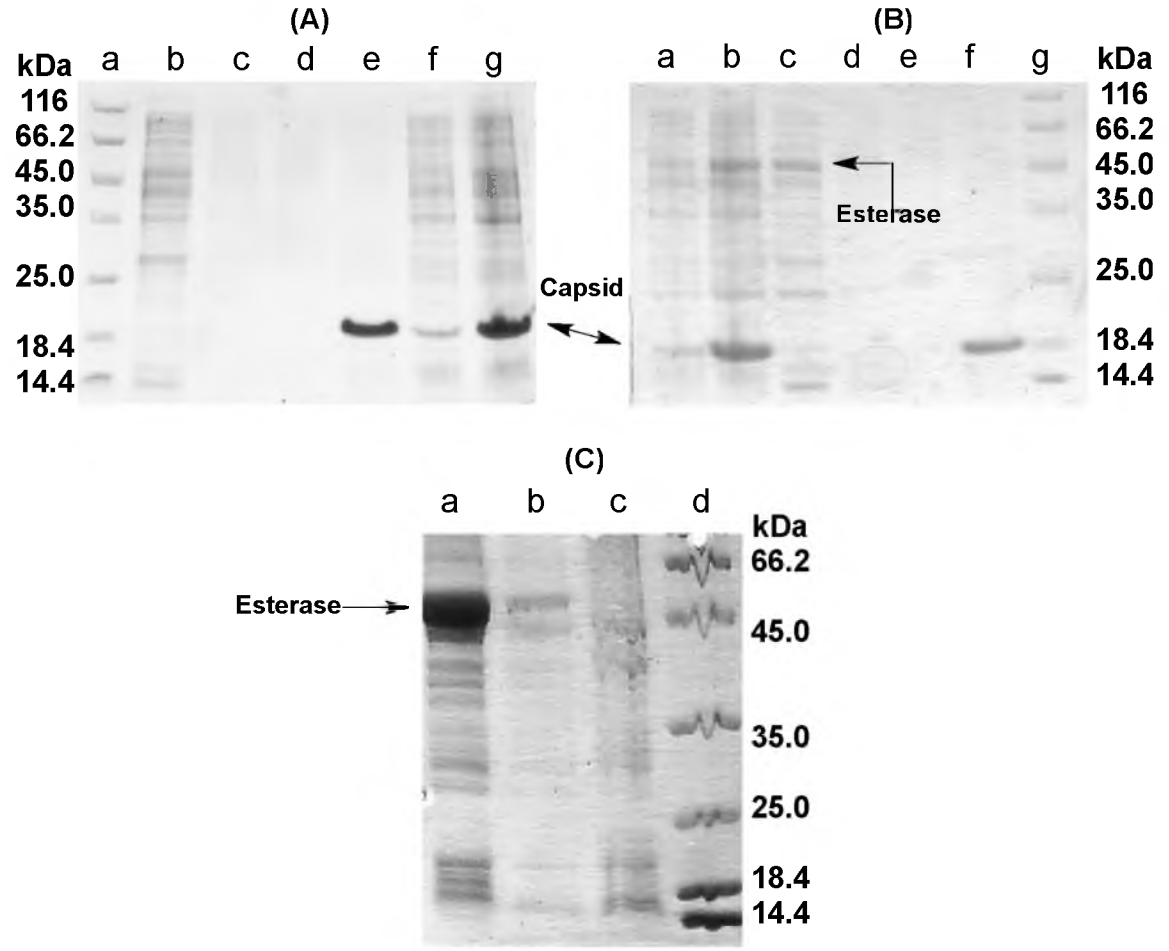

Figure 2.3. SDS-PAGE analysis of protein production and purification. (A) Capsid protein alone. a) Molecular weight standards. b) Flow-through from cell lysate after loading onto Ni-NTA column. c) Column wash with lysis buffer. d) Wash with lysis buffer containing 10 mM imidazole. e) Wash with lysis buffer containing 500 mM imidazole. f) Whole cells before induction. g) Whole cells after induction. (B) Co-production of capsid protein with esterase. a) Whole cells before induction. b) Whole cells after induction. c) Flow-through from cell lysate after loading onto Ni-NTA. d) Column wash with lysis buffer. e) Wash with lysis buffer containing 10 mM imidazole. f) Wash with lysis buffer containing 500 mM imidazole. g) Molecular weight standards. (C) Esterase alone. a) Whole cells after induction. b) Same sample as in a), after dilution to OD_{600} = 0.57. c) Whole cells before induction with OD_{600} = 0.5. d) Molecular weight standards. Molecular weight of both capsid and esterase are 18 kDa and 56 kDa respectively.

similar early eluting peak, which can be attributed to the capsid. The fractions from the size-exclusion column were assayed for esterase activity (Figure 2.4). In the co- produced sample, a peak (fraction 12-14) in esterase activity was observed that corresponded with the elution of the capsid. A second esterase activity peak (fraction 22 and 23) was observed that might reflect either residual free esterase contamination in the sample or some low-level esterase activity of incompletely assembled AaLS-13 itself. In comparison, AaLS-13 produced without esterase showed lower esterase activity in the capsid-containing fractions, and the esterase activity was fairly constant over all protein-containing fractions.

Est55-R_{10} is an efficient catalyst of p-nitrophenyl acetate hydrolysis because it has a catalytic triad in its active site that is well suited to this function[23]. In contrast, AaLS-13 would be expected to be an inefficient esterase because it lacks an organized active site

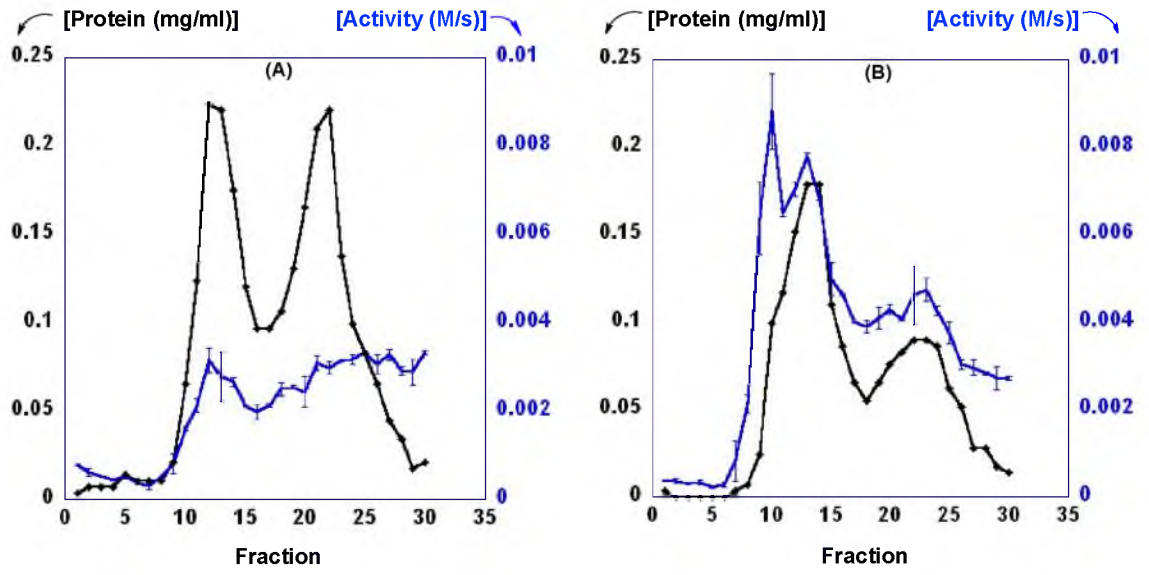

Figure 2.4. Enzyme activity comparison between loaded capsid and empty capsid. (A) Gel filtration chromatograph of AaLS-13 alone and its enzyme activity. (B) Gel filtration chromatograph of AaLS-13 co-produced with Est55-R_{10} and its enzyme activity.

Table 2.1. Specific activity of capsid proteins from AaLS-13 and AaLS-13 co-produced with Est55-R_{10}.

	AaLS-13	AaLS-13 co-produced with Est55-R_{10}
Specific Activity (μmol of product formed/ min/ mg of total protein)	4.0×10^{-3} $\pm 1.9 \times 10^{-3}$	2.6×10^{-1} $\pm 1.3 \times 10^{-1}$

suited to this function. Nonetheless, AaLS-13 may have significant p-nitrophenyl acetate activity because p-nitrophenyl acetate is a highly activated substrate, and the protein

produced sample, a peak (fraction 12-14) in esterase activity was observed that corresponded with the elution of the capsid. A second esterase activity peak (fraction 22 and 23) was observed that might reflect either residual free esterase contamination in the sample or some low-level esterase activity of incompletely assembled AaLS-13 itself. In comparison, AaLS-13 produced without esterase showed lower esterase activity in the capsid-containing fractions, and the esterase activity was fairly constant over all protein-containing fractions.

Est55-R_{10} is an efficient catalyst of p-nitrophenyl acetate hydrolysis because it has a catalytic triad in its active site that is well suited to this function[23]. In contrast, AaLS-13 would be expected to be an inefficient esterase because it lacks an organized active site suited to this function. Nonetheless, AaLS-13 may have significant p-nitrophenyl acetate activity because p-nitrophenyl acetate is a highly activated substrate, and the protein contains many residues capable of acting as nucleophiles, acids, or bases such as histidines, lysines, glutamates, aspartates, the N-terminus, and the C-terminus.

We compared specific activities of the capsid containing fractions for AaLS-13 + Est55-R_{10} and AaLS-13 without esterase to verify that the elevated esterase activity was not due to AaLS-13 itself. From multiple enzyme activity measurements of different protein preparations, we found that the specific activity of the capsid-containing fractions (12-14) for AaLS-13 + Est55-R_{10} was 64-fold higher than that of AaLS-13 produced without esterase (Table 2.1).

2.5 Quantitation of Encapsulated Esterase

The specific activity of free Est55-R_{10} with 100 μM of the substrate was 220 μmol of product formed/ min/ mg of enzyme. If each AaLS-13 capsid is loaded with one Est55-R_{10} molecule, and if the activity of Est55-R_{10} is unaffected by encapsulation, we would expect the specific activity of this hypothetically loaded capsid to be 2.9 μmol of product formed/min/mg of total protein (both the esterase and the capsid, assuming 240 subunits for AaLS-13). Specific activity of the capsid fractions containing AaLS-13 and Est55-R_{10} was 0.26 μmol of product formed/ min/ mg of total protein, which is about 11-fold lower than what would be expected for a loading efficiency of one esterase per capsid. This result suggests that either the catalytic activity of the enzyme inside the capsid has changed, or there is one Est55-R_{10} in every 11 capsids. Therefore, direct quantitation of encapsulated esterase will tell us which one of the two hypotheses is correct.

2.6 Quantitation of Encapsulated Esterase (2)

As an alternative to esterase activity, we turned to SDS-PAGE and mass spectrometry as a means for direct detection and quantitation of Est55-R_{10}. The purified AaLS-13 + Est55-R_{10} complex was analyzed by SDS-PAGE at a high loading of protein

(27 μg). Coomassie blue staining revealed a band whose mobility corresponds to free Est55-R_{10} (Figure 2.5).

The intensity of Est55-R_{10} band indicated that about 30 ng (0.53 pmol) of esterase was present in the sample. Assuming that the amount of AaLS-13 in the sample is close to the total amount of protein, about 6.3 pmols of AaLS-13 were loaded on the gel. This gives ratio of AaLS-13 to Est55-R_{10} as 11.6 : 1. This ratio is close to that expected from the observed activity if the encapsulated Est55-R_{10} is fully active.

There were multiple bands found on the gel from the sample in lane (A). The proteins in all four major bands were identified by liquid chromatography-mass spectrometry (LC-MS/MS). Of these four bands, the highest mobility band was found to be AaLS-13 and the lowest mobility band was assigned as Est55-R_{10}, consistent with their similarities to the purified standards. The other two bands contained a 50S ribosomal protein and a 30S ribosomal protein. These ribosomal proteins are endogenous to and abundant in the *E. coli* cytoplasm and had been previously found to be

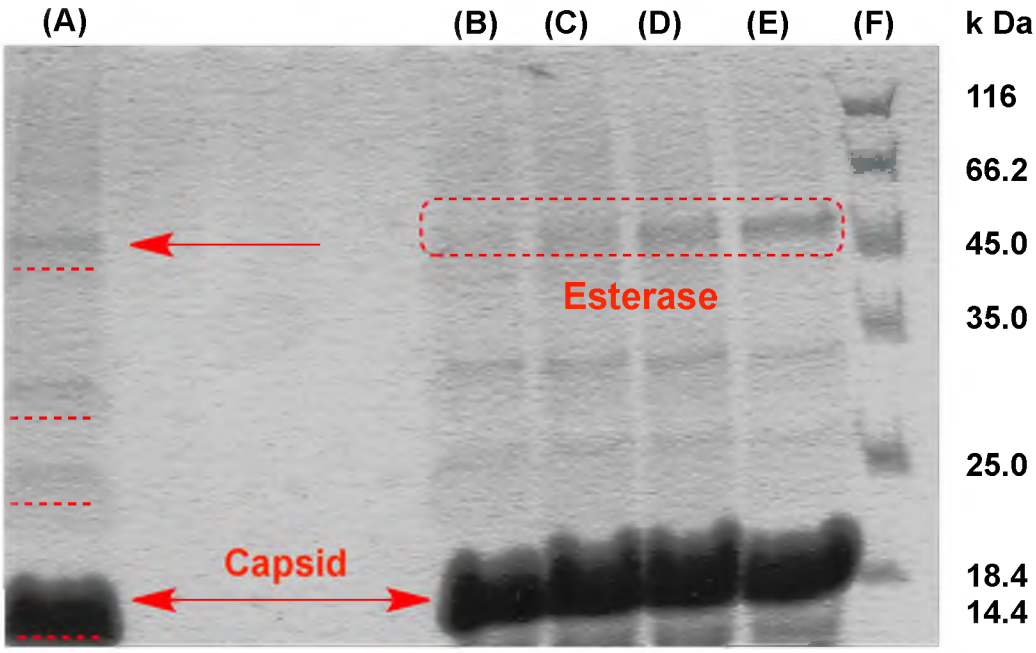

Figure 2.5. Encapsulated esterase detection using SDS-page. (A) AaLS-13 co-produced with Est55-R10 (2.7 x 10^{1} μg). (B) Mixture of capsid (3.4 x 10^{1} μg) and esterase (1.2 x 10^{1} ng). (C) Mixture of capsid (3.4 x 10^{1} μg) and esterase (2.3 x 10^{-2} μg). (D) Mixture of capsid (3.4 x 10^{1} μg) and esterase (4.5 x 10^{-2} μg). (E) Mixture of capsid (3.4 x 10^{1} μg) and esterase (9.0 x 10^{-2} μg). (F) Molecular weight standard.

adventitiously encapsulated by AaLS-13.[24] Consistent with this expectation, these bands were also found in SDS-PAGE analysis of pure AaLS-13 that had been produced in the absence of Est55-R_{10}.

CHAPTER 3

CONCLUSION AND DISCUSSION

Our encapsulated enzyme activity study was carried out by carefully choosing both the capsid and the guest enzyme protein. Est55 has shown its efficient activity towards variable substrates at pH where the capsid is stable. A deca-arginine tag was fused to Est55 for its encapsulation in AaLS-13, and Est55-R_{10} actively hydrolyzed p-nitrophenyl acetate. Encapsulation of the enzyme was done by *in vivo* co-production in *E. coli*. The catalytic activity of the capsid co-produced with the enzyme was dramatically higher than that of the empty capsid. The loaded capsid showed 64-fold higher specific activity than that of the empty capsid. SDS-PAGE analysis of concentrated loaded capsid sample showed a protein band that corresponds to free Est55-R_{10}. Comparison of the Est55-R_{10} gel band intensity to purified standards of free Est55-R_{10} gave a rough estimate of the capsid loading that corresponds to one esterase per 11 capsids. This estimate is in gratifying agreement with an independent determination of capsid loading based on catalytic activity.

There is uncertainty about the subunit stoichiometry of the AaLS-13 capsid. AaLS-13 was generated by rational design and directed evolution. As a consequence, five residues at subunit interfaces are mutated. Some of the mutations eliminated previously established salt bridges in the subunit interaction site of AaLS-wt. The diameter of AaLS-

13 is 34.7 ± 3.4 nm, which is slightly larger than that of AaLS-neg (28.6 ± 2.6 nm).[24] We assume the expansion of the capsid may be due to either increasing the number of subunits in the capsid from 180 to 240 or an alternative packing of 180 subunits. To answer the question, we are currently using analytical ultra-centrifugation (AUC) to estimate molecular weight of the AaLS-13 capsid.

The activity of AaLS-13 co-produced with Est55-R_{10} can be compared with that of other controls (AaLS-13 co-produced with Est55 and AaLS-wt co-produced with Est55-R_{10}). These controls lack charge complementarity either from the capsid or from the enzyme. Their loading capability should not be as efficient as our engineered nanoreactor system. Thus the esterase activity with p-nitrophenyl acetate of these controls would expected to be lower than that of AaLS-13 co-produced with Est55-R_{10}.

The porosity of the capsid is the important enzyme activity-regulating factor of our nanoreactor. Assuming the five-fold symmetric pores in the AaLS-13 are the only entries for substrates, the encapsulated esterase should be inactive with substrates too large to fit through the pore (Table 3.1) (Figure 3.1). The determination of the molecular weight cut-off for capsid will inform efforts to develop more sophisticated nanoreactors.

Table 3.1. Varying size of substrates.

Substrates	Molecular Weight
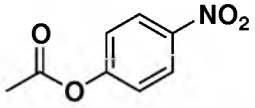 p-nitrophenyl acetate	181 Da
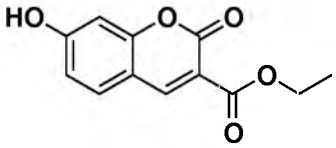 Ethyl-7-hydroxy-2-oxo-2H-chromene-3-carboxylate	234 Da
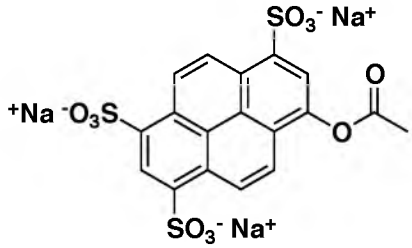 Sodium 8-acetoxypyrene-1,3,6-trisulfonate	566 Da
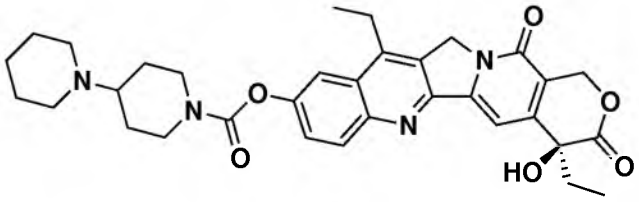 CPT-11	586 Da

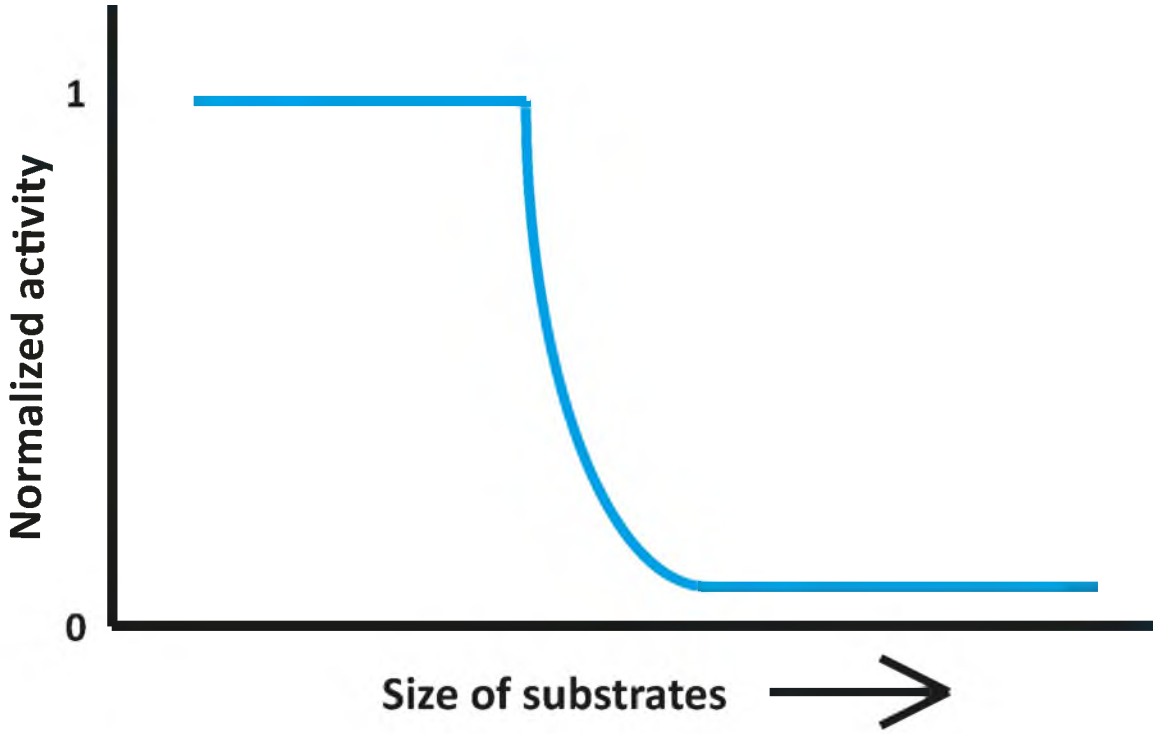

Figure 3.1. Estimated enzyme activity vs size of substrates.

CHAPTER 4

MATERIALS AND METHODS

Cell culture media, salts and chemical reagents were purchased from Sigma-Aldrich, Fisher scientific, Pierce biotechnology and Bio-rad. The protein analysis and identification were done by the Mass spectrometry and Proteomics Core Facility at University of Utah.

4.1 Protein Production and Purification

For overproduction of proteins, calcium competent BL21 DE3 *E. coli* cells were transformed with pMG-AaLS-13, pACYC-Est55-R10, and both at 42 °C for 45 s. Cell cultures were grown at 37 °C and 250 rpm in LB medium (500 ml) with ampicilin (100 mg/L) until the $O.D_{600}$ reached 0.6. For co-production with Est55-R_{10} or Est55-R_{10} alone chloramphenicol (100 mg/L) was supplemented. The cultures were induced with 0.1 mM final concentration of IPTG at 37 °C and 250 rpm for 4 h. After the induction, the cells were harvested by centrifugation at 2960 xg and 4 °C for 10 min.

The cell pellets were resuspended in 20 ml lysis buffer (50 mM sodium phosphate, 100 mM sodium chloride, pH 8.0) and lysed by incubation with lysozyme (5 mg), RNase (0.6 mg), and ten units of DNase in ice followed by sonication (45 amp, total 3 min of sonication in ice: 1 min pulse on followed by 1 min rest). Cell lysate

of either the capsid alone or the capsid co-produced with the esterase were cleared by centrifugation (12000 xg for 30 min at 4 °C) and loaded onto 10 ml Ni^{2+}-NTA agarose resin (Qiagen) that had been equilibrated with a lysis buffer. Cell lysate of the esterase alone skipped Ni^{2+}-NTA purification. After washing with both a lysis buffer (50 mL) and a lysis buffer containing 10 mM and 40 mM imidazole (50 mL), capsids were eluted with a lysis buffer containing 500 mM imidazole (15 mL) and the collection tube contains 2 mL of 0.5 M EDTA. Protein purity was assessed by SDS-PAGE. Protein concentrations were determined using the Coomassie Plus Protein Assay Reagent (Thermo Scientific).

4.2 Gel Filtration Chromatography (Size Exclusion) and Ion-Exchange Column

The AaLS-13 capsid and AaLS-13 co-produced with Est55-R_{10} were further purified by gel filtration chromatography using a HiPrep 16/60 Sephacryl S-400HR columns (GE healthcare). The protein was loaded to the column pre-equilibrated with gel filtration running buffer (50 mM sodium posphate, 300 mM NaCl, and 5 mM EDTA, pH 8). The running temperature was 4 °C at a flow rate of 0.5 ml/min.

Crude Est55-R_{10} was loaded onto an cation-exchange MONO S™ 5/50 column (GE healthcare). The column was pre-equilibrated with low-salt buffer A (50 mM sodium phosphate, 50 mM sodium chloride, and 5 mM EDTA, pH 8). The column bound Est55-R_{10} was eluted with a gradient from 0 to 100% ion-exchange buffer B (50 mM sodium phosphate, 2 M NaCl, and 5 mM EDTA, pH 8) over 40 mL at 4 °C.

4.3 Enzyme Activity

All experiments were run in duplicate, and all kinetic data analyzed with respect to the enzyme concentration except the capsid co-produced with Est55-R_{10} that were in respect to the total protein concentration (enzyme plus capsid). The activity and kinetics of purified AaLS-13 (11 μM), AaLS-13 co-produced with Est55-R_{10} (5.3 μM), and free Est55-R_{10} (1.2 nM) were analyzed with the substrate p-nitrophenyl acetate (Sigma-Aldrich) using a U-3310 spectrophotometer, HITACHI (absorbance 405 nm, 1500 s read time). For determinations of enzyme kinetics, several different concentrations of the substrate (25, 50, 100, 200, 400, 800 μM) were prepared in ethanol by serial dilutions: 5 μl of each different substrate concentration were added to 1 ml of enzyme solution (50 mM phosphate, 100 mM NaCl, 5 mM EDTA, pH 8) of Est55-R_{10} at 30 °C and read immediately. Concentration of each substrate was recalculated using Beer-Lambert law, $A = \varepsilon lc$ by taking endpoint absorbance corresponding to 100% product and extinction coefficient of product ($\Delta\varepsilon = 17800\ M^{-1}cm^{-1}$).

Enzyme activity of AaLS-13 and AaLS-13 with Est55-R_{10} were measured for fractions (1 to 30) from the gel filtration column. Reaction conditions were identical to the free Est55-R_{10}.

4.4 Encapsulated Esterase Detection

Concentrated capsid sample (AaLS-13 co-produced with Est55-R_{10}) was loaded on SDS-page gel (12% acrylamide, 150 V, for 60 min). Four of protein bands were analyzed and identified by LC-MS/MS in mass spectrometry and proteomics core facility at University of Utah.

REFERENCES

1. Heddle, J. G., *J. Nano. Sci. Application*, **2008**, 1, 67-78

2. Yeates, T. O., Crowley, C. S., and Tanaka, S., *Annu. Rev. Biophys.*, **2010**, 39, 185-205

3. Tanaka, S., Sawaya, M. R., Yeates, T. O., *Science*, **2010**, 327, 81-84

4. Yamada, T., Iwasaki, Y., Tada, H., Iwabuki, H., Chuah, M. K. L., Vanden Driessche, T., Fukuda, H., Kondo, A., Ueda, M., Seno, M., Tanizawa, K., Kuroda, S., *Nat. Biotechnol.*, **2003**, 21, 885-890

5. Abbing, A., Blaschke, U. K., Grein, S., Kretschmar, M., Stark, C. M. B., this, M. J. W., Walter, J., Weigand, M., Woith, D. C., Hess, J., Reiser, C. O. A., *J. Biol. Chem.*, **2004**, 279, 27410-27421

6. Schaffer, D. V., Koerber, J. T., Lim, K.-I., *Annu. Rev. Biomed. Eng.*, **2008**, 10, 169-194.

7. Stephanopoulos, N., Tong, G. J., Hsiao, S. C., Francis, M. B., J. *Am. Chem. Soc. Nano.*, **2010**, 4, 6014-6021

8. Aime, S., Frullano, L., Geninatti Crich, S., *Angew, Chem., Int. Ed.*, **2002**, 41, 1017-1019

9. Uchida, M., Flenniken, M. L., Allen, M., Willits, D. A., Crowley, B. E., Brumfield, S., Willis, A. F., Jackiw, L., Jutila, M., Young, M. J., Douglas, T., *J. Am. Chem. Soc.*, **2006**, 128, 16626-16633

10. Hooker, J. M., Datta, A., Botta, M., Raymond, K. N., Francis, M. B., *Nano Lett.*, **2007**, 7, 2207-2210

11. Liepold, L. L., Abedin, M. J., Buckhouse, E. D., Frank, J. A., Young, M. J., Douglas, T., *Nano Lett.*, **2009**, 9, 4520-4526

12. Uchida, M., Kang, S., Reichhardt, C., Harlen, K., Douglas, T., *Biochim. Biophys.*, **2010**, 1800, 834-845

13. Douglas, T., Young, M., *Adv. Mater.*, **1999**, 11, 679-681

14. Minten, I., Claessen, V., Blank, K., Rowan, A., Nolte, R., Cornelissen, J., *Chem. Sci.*, **2011**, 2, 358-362

15. Fiedler, J., Brown, S., Lau, J., Finn, M., *Angew, Chem., Int. Ed.*, **2010**, 49, 9648-9651

16. Comellas-Aragones, M., Engelkamp, H., Claessen, V., Sommerdijk, N., Rowan, A., Christianen, P., Maan, J., Verduin, B., Cornelissen, J., Nolte, R., *Nat, Nanotechnol.*, **2007**, 2, 635-639

17. Nasseau, M., Boublik, Y., Meier, W., Winterhalter, M., Fournier, D., *Biotechnol. Bioeng.*, **2001**, 75, 615-618

18. Kimura, M., Kato, M., Muto, T., Hanabusa, K., Shirai, H., *Macromolecules*, **2000**, 33, 1117-1119

19. Zhang, X., Meining, W., Fischer, M., Bacher, A., Ldenstein, R., *J. Mol. Biol.*, **2001**, 306, 1099-1114

20. Persson, K., Schneider, G., Jordan, D. B., Viitanen, P. V., Sandalova, T., *Protein Sci.*, **1999**, 8, 2355-2365

21. Ladenstein, R., Ritsert, K., Huber, R., Richter, G., Bacher, A., *Eur. J. Biochem.*, **1994**, 223, 1007-1017

22. Seebeck, F. P., Woycechowsky, K. J., Zhuang, W., Rabe, J. P., Hilvert, D., *J. Am. Chem. Soc.*, **2006**, 14, 4516-4517

23. Szeltner, Z., Polgar, L., *J. Biol. Chem.*, **1996**, 271, 32180-32184

24. Worsdorfer, B., Woycechowsky, K. J., Hilvert, D., *Science*, **2011**, 331, 589-592

25. Hong, K. H., Jang, W. H., Choi, K. D., *Agric. Biol. Chem.*, **1991**, 55, 2839-2845

26. Ewis, H. E., Abdelal, A. T., Lu, C.-D., *Gene*, **2004**, 329, 187-195

27. Kim, Y.-O., Park, I.-S., Kim, H.-K., Nam, B.-H., Kong, H. J., Kim, W.-J., Kim, D.-G., Kim, K.-K., Lee, S.-J., *J. Gen. Appl. Microbiol.*, **2011**, 57, 357-364

28. Hong, K.-H., Jang, W.-H., Choi, K.-D., Yoo, O.-J., *Agric. Biol. Chem.*, **1991**, 55, 2839-2845

29. H.-N. Chen and M. Fetherolf, unpublished result, **2009**